

On the Way to Selective PARP-2 Inhibitors. Design, Synthesis, and Preliminary Evaluation of a Series of Isoquinolinone Derivatives

Roberto Pellicciari,^{*,[a]} Emidio Camaioni,^[a] Gabriele Costantino,^[a] Laura Formentini,^[b] Paola Sabbatini,^[a] Francesco Venturoni,^[a] Gökçen Eren,^[a] Daniele Bellocchi,^[a] Alberto Chiarugi,^[b] and Flavio Moroni^[b]

PARP-1 and PARP-2 are members of the family of poly(ADP-ribose)polymerases, which are involved in the maintenance of genomic integrity under conditions of genotoxic stimuli. The different roles of the two isoforms under pathophysiological conditions have not yet been fully clarified, and this is partially due to the lack of selective inhibitors. We report herein the synthesis and

preliminary pharmacological evaluation of a large series of isoquinolinone derivatives as PARP-1/PARP-2 inhibitors. Among them, we identified the 5-benzoyloxyisoquinolin-1(2H)-one derivative as the most selective PARP-2 inhibitor reported so far, with a PARP-2/PARP-1 selectivity index greater than 60.

Introduction

Maintenance of genomic integrity under acute or chronic genotoxic stimuli is achieved by a variety of mechanisms, among which poly(ADP-ribosylation) plays a fundamental role. Poly(ADP-ribosylation) is a covalent post-translational modification operated by members of a family of at least 17 genes,^[1] the products of which remain, in part, elusive in their function and mechanisms of action. The founding member of the family is poly(ADP-ribose)polymerase-1 (PARP-1). PARP-1 is a chromatin-bound nuclear enzyme which, upon activation by a DNA single-strand break, uses NAD⁺ as a co-substrate to poly(ADP-ribosyl)ate acceptor proteins. Thus, in the presence of mild DNA damage, PARP-1 becomes activated and starts poly(ADP-ribosyl)ating nuclear proteins such as histones and polymerases, thus allowing recruitment of DNA repair machinery and subsequent recovery from damage. However, if the damage is too severe and cannot be repaired, PARP-1 hyperpoly(ADP-ribosyl)ates acceptor proteins, thus depleting ATP which leads to energy crisis and cell death.^[2,3] In this respect, PARP-1 can be considered the executioner of cell death in conditions of severe insult; its shut-down, through molecular or pharmacological intervention, can prevent degeneration in a variety of tissues and organs, including brain, heart, and pancreas. In particular, PARP-1 inhibitors have been proposed as clinical candidates for a variety of acute and chronic diseases, including cancer, brain and heart ischemia, diabetes, and inflammation.^[4] The involvement of PARP-1 in cerebral ischemia has received the first substantial validation from the observation that deletion of the *PARP-1* gene in mouse produces phenotypes highly resistant to excitotoxicity and stroke.^[5]

Of the 17 members of the PARP family, there is only one other enzyme, termed PARP-2, which is activated by DNA strand breaks and is endowed with poly(ADP-ribose)polymerase activity. Indeed, PARP-2 was discovered as a result of the

detection of residual DNA-dependent PARP activity in PARP-1-deficient mouse fibroblasts.^[6,7] The PARP-2 expression pattern matches that of PARP-1, and the two enzymes co-localize in the nucleus.

The presence of two PARP enzymes that are both activated by DNA breaks, and which are found in the same cells and tissues raises questions about their individual roles under pathophysiological conditions. Apparently, the two enzymes have overlapping and redundant functions. *PARP-1*^{-/-} animals have residual yet appreciable PARP activity upon genotoxic stimulus.^[8] It should be noted, however, that under conditions of severe DNA damage, the cell executioner role of PARP-1 cannot be taken up by PARP-2 in PARP-1-deficient animals, which are therefore substantially resistant to stroke or excitotoxicity. Along the same lines, it was observed that after focal cerebral ischemia, brain levels of NAD⁺ in *PARP-1*^{-/-} mice were similar to those in animals treated with a nonspecific PARP inhibitor, suggesting that NAD⁺ depletion is mainly caused by the activation of PARP-1, and not other isoforms.^[9] Nevertheless, if *PARP-2*^{-/-} mice are subjected to focal ischemia (MCAO) and reperfusion, a decrease in infarct volume of up to 40% is

[a] Prof. R. Pellicciari, Prof. E. Camaioni, Prof. G. Costantino,⁺ Dr. P. Sabbatini, Dr. F. Venturoni, Dr. G. Eren, Dr. D. Bellocchi
Dipartimento di Chimica e Tecnologia del Farmaco
Università di Perugia, Via del Liceo 1, 06123 Perugia (Italy)
Fax: (+39) 075-585-5161
E-mail: rp@unipg.it

[b] Dr. L. Formentini, Prof. A. Chiarugi, Prof. F. Moroni
Dipartimento di Farmacologia Clinica e Preclinica
Università di Firenze, Viale Pieraccini 6, 50139 Firenze (Italy)

[*] Current address: Dipartimento Farmaceutico
Università di Parma, Viale Usberti 27A Campus, 43100 Parma (Italy)

Supporting information for this article is available on the WWW under <http://www.chemmedchem.org> or from the author.

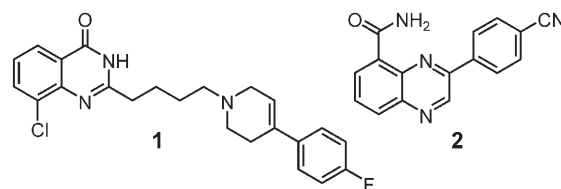
observed.^[10] No clear explanation can be given for this, as it does not correlate with the level of poly(ADP-ribosylation) (PAR) mediated by PARP-2 under physiological conditions, which is no greater than 10%.^[8,11] It can be speculated that deletion of PARP-2 may hamper the ability to form heterodimers with PARP-1, thus causing a global decrease in PAR activity. However, the total PAR activity of *PARP-2*^{-/-} animals has not been measured against wild-type, and so definitive conclusions cannot be drawn.^[10] When *PARP-2*^{-/-} animals are subjected to global ischemia and resuscitation, a significant increase in neuronal loss is observed in the hippocampus, thus highlighting PARP-2 as a mandatory survival factor to mitigate delayed cell death in the hippocampus. Again, no clear hypothesis can be put forward as to why PARP-2 deletion should result in increased toxicity. Notably, however, the effect is observed only in the hippocampus, which is known to develop delayed neuronal death relative to other vulnerable regions. A potential mechanism for the delay in neuronal death may involve loss of DNA repair activity.

A recent report has shown PARP-2, but not PARP-1, is an important mediator of T-cell survival during thymopoiesis by preventing the activation of DNA-damage-dependent apoptotic responses.^[12] Furthermore, in accordance with the proposed role of PARPs as epigenetic modulators of physiological function, PARP-2 has been implicated in both meiotic and post-meiotic processes, as PARP-2-deficient mice exhibit severely impaired spermatogenesis.^[13]

Altogether, these data clearly indicate that knock-out animals do not provide definitive information regarding the differential physiological roles of PARP-1 and PARP-2, possibly because of the intervention of compensatory mechanisms. This observation strongly puts forward the need for selective PARP-1/PARP-2 inhibitors, not only as potential preclinical candidates for specific indications, but also for use as pharmacological tools to elucidate the role of each isoform.

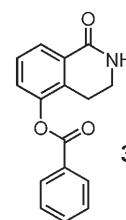
PARP-1 and PARP-2 share sequence identity, which is relatively low in the DNA binding domain, but more pronounced in the catalytic domain (70%). This implies that the two isoforms may interact with different target genes and may poly-(ADP-ribosyl)ate different acceptor proteins; nevertheless, selective PARP-1 or PARP-2 inhibitors are still missing. Moreover, in the consideration that PARP-2 assays have been made available only recently, many reported "PARP-1" inhibitors would be more appropriately classified as "PARP" inhibitors unless and until their selectivity between the two isoforms has been proven.

There are only a few known examples of chemotypes that have appreciable isoform selectivity. Thus, through a high-throughput screen, Iwashita and co-workers^[14,15] recently identified a series of quinazolinone and quinoxaline derivatives that displayed some selectivity toward PARP-1 and PARP-2, respectively. In particular, quinazolinone **1** was 39-fold more active at PARP-1 than at PARP-2 ($IC_{50\text{PARP-2}} = 500 \text{ nM}$; $IC_{50\text{PARP-1}} = 13 \text{ nM}$), whereas quinoxaline **2** was 13-fold more active at PARP-2 ($IC_{50\text{PARP-1}} = 101 \text{ nM}$; $IC_{50\text{PARP-2}} = 8 \text{ nM}$). Both quinazolinone **1** and quinoxaline **2** encompass the canonical PARP pharmacophore, constituted by a benzamide moiety in an *anti* con-



formation. The source of isoform selectivity has to be ascribed, therefore, to their different abilities to interact with enzyme regions close to the catalytic pocket.

As a part of our research project devoted to the design and synthesis of PARP inhibitors as potential anti-excitotoxic agents, we previously reported a series of isoquinolinone derivatives active as PARP-1 inhibitors.^[16,17] Re-screening that series of derivatives on an *in vitro* assay for recombinant mouse PARP-2 activity allowed us to identify 5-benzoyloxy-3,4-dihydroisoquinolin-1(2*H*)-one (**3**) as a moderately selective PARP-2 inhibitor, with an IC_{50} value of $0.8 \mu\text{M}$ against PARP-2, compared with an IC_{50} value of $13 \mu\text{M}$ toward PARP-1.



On the basis of this first indication, a library of substituted isoquinolinone derivatives was designed around compound **3**, synthesized by applying parallel solution-phase synthesis, and evaluated for PARP-1/PARP-2 inhibitors; the results are reported herein.

Synthesis Design

A large series of modifications was designed around scaffold **3** by preserving the canonical PARP pharmacophore constituted by the conformationally constrained benzamide moiety (Table 1 and Table 2). Thus, 1) the benzoyl ring was decorated with fluorine and chlorine atoms in the *ortho*, *meta*, and *para* positions (compounds **19–24**, Table 1); the *para* position was then further investigated by introduction of a bromine atom (in **25**), alkyl and aryl groups (in **26–32**), or electron-withdrawing groups (compounds **33** and **34**). 2) The phenyl ring itself was replaced by furan and thiophene rings (compounds **35** and **36**, respectively), and by the fully saturated cyclohexyl ring (compound **37**). 3) The linkage between the distal aromatic ring and the dihydroisoquinolinone moiety was substituted by various spacers to afford the corresponding benzyl, acetophenone, and cinnamyl derivatives (compounds **38–50**). 4) Other dihydroisoquinolinone derivatives in which the ester function is conformationally constrained into a rigid heterocyclic system were also prepared (compounds **51–53**). 5) Isoquinolinone derivatives were prepared as well (compounds **54** and **55**). 6) Finally, the dihydroisoquinolinone moiety was modified, through ring reduction (from six-membered to five-membered ring, **56**) and ring opening (compounds **57–59**, Table 2).

Chemistry

As summarized in Scheme 1, derivatives **3** and **19–59** were synthesized by nucleophilic substitution between 5-hydroxy-

Table 1. Structures and residual PARP-1 and PARP-2 activities in the presence of compounds **3** and **19–55**.

Compd	R	Activity [%] ^[a]			
		PARP-1		PARP-2	
		Exp. 1	Exp. 2	Exp. 1	Exp. 2
control	–	100	100	100	100
3		52.0	46.2	32.2	25.7
19		52.1	50.8	21.8	22.9
20		34.6	35.6	18.9	17.1
21		68.8	77.3	64.3	74.2
22		47.6	46.6	23.9	29.6
23		36	35.1	18.3	17.7
24		46.8	47.3	29.1	28.2
25		46.1	48.5	36.7	31.4
26		45.8	42.8	44.1	47.1
27		59.3	60.2	38.2	33.9
28		67.2	66.3	38.2	33.9
29		49.7	60.1	35.2	28.3
30		92.2	91.3	61.5	64.2
31		82.9	84.1	65.6	64.5
32		70.3	92.4	58.4	66.8

Table 1. (Continued)

Compd	R	Activity [%] ^[a]			
		PARP-1		PARP-2	
		Exp. 1	Exp. 2	Exp. 1	Exp. 2
33		46.2	29.2	12.8	14.1
34		16.1	12.5	11.3	5.9
35		25.2	40.2	25.3	36.6
36		46.8	43.9	22.1	23.9
37		52.1	51.1	41.8	41.8
38		53.9	55.6	44.4	57
39		70.2	73.9	69.2	80.8
40		86.3	83.1	43.9	98.6
41		84.5	80.1	96.7	89.7
42		82.4	83	56.4	30.35
43		44.1	39.5	24.8	37.6
44		34.1	43.4	19.3	21.6
45		25.9	31.3	21.4	20.8
46		41.6	39.5	17.1	34.5
47		62.7	65.6	23.8	19.2
48		54.1	49.2	25.6	18.5
49		27.7	36.1	17.2	21.6
50		36.2	47.6	25.6	36.1

Table 1. (Continued)

Compd	R	Activity [%] ^[a]			
		PARP-1		PARP-2	
		Exp. 1	Exp. 2	Exp. 1	Exp. 2
51		39.6	42.7	33.6	30
52		86.8	83.9	79.5	84.5
53		82.7	82.6	67.1	61.5
54		37.8	47.9	5.2	6.1
55		33.8	42.1	22.1	28.7

[a] Single dose at 10 μM ; data represent the mean of duplicates from experiments 1 and 2.

3,4-dihydroisoquinolin-1(2*H*)-one (**4**), 5-hydroxyisoquinolin-1(2*H*)-one (**5**), 4-hydroxyisoindolinone (**6**), 3-hydroxy-2-methylbenzamide (**7**), 3-hydroxy-*N*-methylbenzamide (**8**), 3-hydroxybenzamide (**9**), and the suitable aromatic acyl chlorides, bromoacetophenones, and heterocyclic halide reagents using a parallel synthesis technique. 5-hydroxy-3,4-dihydroisoquinolin-1(2*H*)-one (**4**)^[18] was prepared by starting from the commercially available 4-hydroxyindan-1-one (**10**) via a modified Smith rearrangement optimized to obtain the desired regioisomer **4** in 57% yield, with a 7:3 ratio with respect to **11**^[19] (Scheme 2). The 5-hydroxyisoquinolin-1(2*H*)-one (**5**)^[20] was obtained in 34% yield from 5-isoquinoline sulfonic acid (**12**) by submitting **12** to alkaline fusion^[20] (Scheme 3).

4-hydroxyisoindolin-1(1*H*)-one (**6**)^[21] was prepared from 2-methyl-3-methoxy benzoic acid (**13**) as shown in Scheme 4. Thus, **13** was treated with thionyl chloride and methanol to obtain the corresponding methyl ester **14** in quantitative yield. Treatment of **14** with *N*-bromosuccinimide under radical conditions afforded, in 65% yield, the corresponding brominated derivative **15**, which was then cyclized in the presence of methanolic ammonia to obtain the corresponding isoindolinone derivative **16** in quantitative yield. The latter was finally demethylated by treatment with boron tribromide to obtain the desired 4-hydroxyisoindolin-1(1*H*)-one (**6**) in 73% yield.

Compound **7**^[18] was synthesized, as outlined in Scheme 5, by starting from 2-methyl-3-methoxybenzoic acid (**13**). Thus **13** was first treated with ammonia in the presence of carbonyldiimidazole to obtain the corresponding benzamide intermediate **17**^[18] in 85% yield. Treatment of **17** with boron tribromide afforded the desired compound 3-hydroxy-2-methylbenzamide (**7**) in 79% yield.

Table 2. Structures and residual PARP-1 and PARP-2 activities in the presence of benzyloxy derivatives **56–59**.

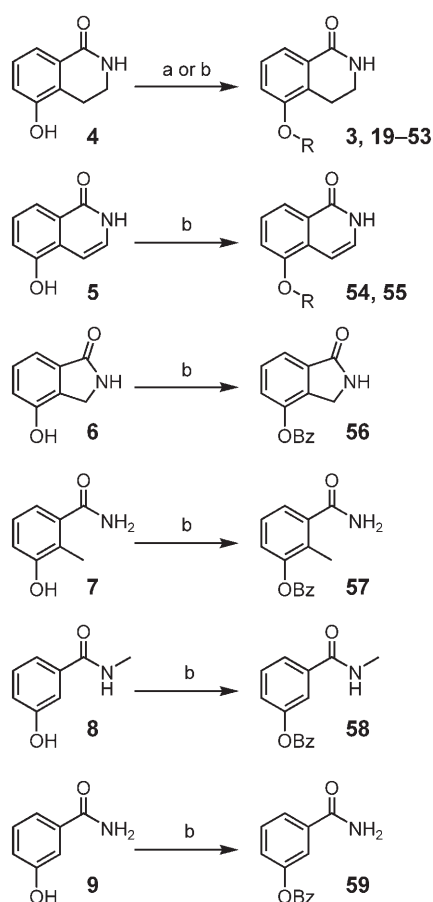
Compd	Structure	Activity [%] ^[a]			
		PARP-1		PARP-2	
		Exp. 1	Exp. 2	Exp. 1	Exp. 2
56		66.1	68.9	56.4	46.1
57		74.6	66	73.7	57.4
58		91.9	88.5	80.2	87.1
59		78.1	80.9	61.3	66.5

[a] Activity at 10 μM ; data represent the mean of duplicates from experiments 1 and 2.

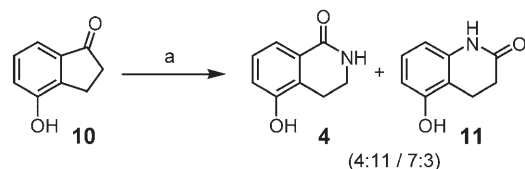
Benzamide derivatives **8** and **9** were synthesized by starting from 3-hydroxybenzoic acid (**18**), as depicted in Scheme 6. Thus, **18** was treated with thionyl chloride, methylamine, or ammonia to give the corresponding 3-hydroxy-*N*-methylbenzamide (**8**)^[22] in 38% yield and 3-hydroxybenzamide (**9**)^[22] in 40% yield.

Biological Results

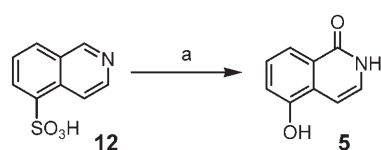
The newly synthesized compounds were preliminarily screened at a concentration of 10 μM against recombinant bovine PARP-1 and mouse PARP-2 by monitoring the residual poly(ADP-ribose) transferase activity. The results are summarized in Tables 1 and 2, and their inspection allowed us to delineate a preliminary SAR profile for the new derivatives. In particular, the following conclusions can be drawn: First, the distal aromatic moiety is amenable to a variety of modifications. Thus, the introduction of a chlorine or fluorine atom in the *ortho* or *meta* positions of the distal aromatic ring enhanced inhibitory potency at 10 μM while maintaining the selectivity profile of the parent compound (**19**, **20**, **22**, and **23**), whereas substitution at the *para* position gave contrasting results, as chlorine, alkyl, or aryl groups markedly decreased potency, while fluorine and small



Scheme 1. Reagents and conditions: a) 1. NaOH, MeOH, reflux, 2. R-X, H₂O, *n*Bu₄NHSO₄, reflux; b) R-X, K₂CO₃, DMF. Bz = benzoyl group; R groups: see Table 1.

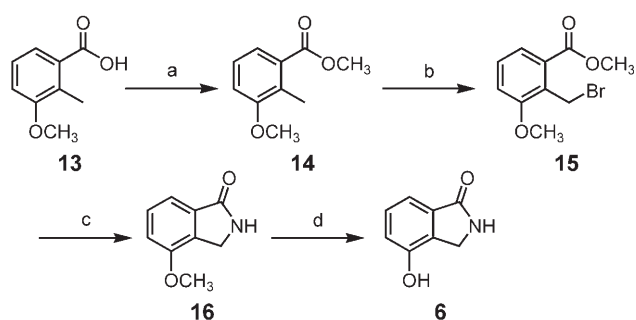


Scheme 2. Reagents and conditions: a) NaN₃, CCl₃CO₂H, 90 °C.

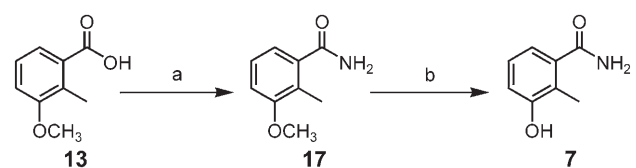


Scheme 3. Reagents and conditions: a) KOH, 230 °C.

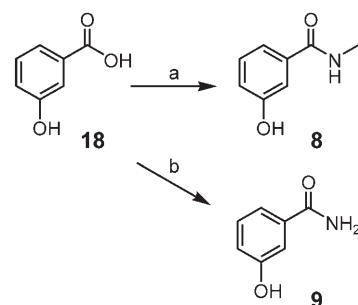
electron-withdrawing groups increased potency at both PARP-1 and PARP-2 isoforms (**24**, **25**, **33**, and **34**). Potential bioisosteric replacement of the distal phenyl ring also gave contrasting results. Thus, replacement of the phenyl by a thiophene ring provided derivative **36**, with properties similar to that of the parent compound **3**, whereas furan **35** and cyclohexyl compound **37** led to complete loss of selectivity and decreased inhibitory activity. The nature of the linker between



Scheme 4. Reagents and conditions: a) 1. SOCl₂, toluene, reflux, 2. MeOH, 0 °C; b) NBS, AIBN, CCl₄, room temperature; c) NH₃, MeOH, reflux; d) BBr₃, CH₂Cl₂, reflux. AIBN = 2,2'-azobisisobutyronitrile, NBS = *N*-bromosuccinimide.



Scheme 5. Reagents and conditions: a) 1. CDI, THF, room temperature, 2. NH₃, THF, reflux; b) BBr₃, CH₂Cl₂, reflux. CDI = 1,1'-carbonyldiimidazole.



Scheme 6. Reagents and conditions: a) 1. SOCl₂, toluene, reflux, 2. CH₃NH₂, THF, 0 °C → room temperature; b) 1. SOCl₂, toluene, reflux, 2. NH₃, THF, 0 °C → room temperature.

the distal aromatic moiety and the isoquinolinone ring also impacts activity. Replacement of the benzoyl moiety with a benzyl group (in **38** and **39**) leads to complete loss of selectivity and decreased inhibitory activity. Sulfonic and cinnamyl derivatives **40–42** were inactive, whereas the introduction of a methylene spacer between the carbonyl and phenyl groups led to compound **43**, endowed with moderate PARP-1 and PARP-2 inhibitory activity. Compound **44**, which has an acetophenone group linked to the oxygen atom at the 5-position in the dihydroisoquinolinone scaffold, displayed interesting selectivity and potency similar to the parent derivative **2**. Further elaboration around this scaffold indicates that acetophenone derivatives substituted with halides (in **45** and **46**) are nonselective, whereas substitution with electron-withdrawing groups (in **47–49**) yields compounds that maintain inhibitory activity and selectivity. Among the various heterocycles introduced in the distal position, only compound **51**, bearing a benzoisothia-

zole, showed some selectivity and activity toward PARP-2. Modifications at the isoquinolinone nucleus were also introduced. Thus, the isoindolinone derivative **56** and open analogues **57–59** were essentially inactive, while in contrast, isoquinolinone derivatives **54** and **55** were the most potent and selective among this series.

Given these results, a subset of the new derivatives was selected for further biological characterization with the aim of further characterizing the structure–activity relationships. Thus, full dose–response curves for PARP-1/PARP-2 inhibition were calculated for compounds **3**, **19**, **23**, **44**, **47**, **51**, **54**, and **55**, along with PJ34 (2-(dimethylamino)-*N*-(6-oxo-5,6-dihydrophenanthridin-2-yl)acetamide,^[23] **60**) and DPQ (5-(4-piperidinylbutoxy)-3,4-dihydroisoquinolin-1(2*H*)-one,^[18] **61**) as reference compounds. The corresponding IC₅₀ values are reported in Table 3, allowing a more precise estimate of the selectivity between the two isoforms.

Analysis of the results reported in Table 3 indicates that PJ34 and DPQ, broadly employed as reference compounds for PARP inhibition, actually do not discriminate between the two main PARP isoforms. Elaborations around the dihydroisoquinolinone

Table 3. PARP-1 and PARP-2 inhibitory activity of selected compounds.^[a]

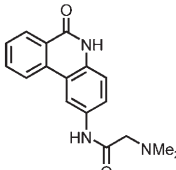
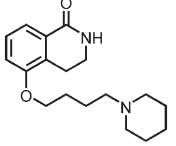
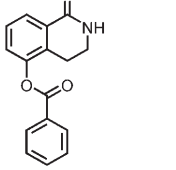
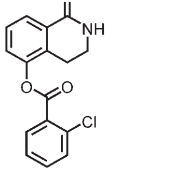
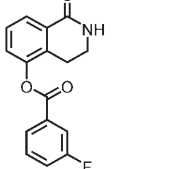
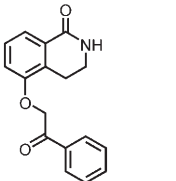
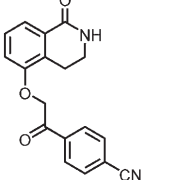
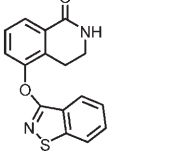
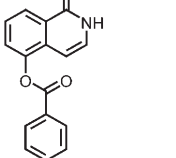
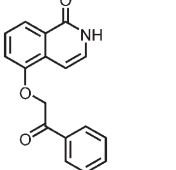
Compound	IC ₅₀ [μM]		Selectivity PARP-1/PARP-2	
	PARP-1	PARP-2		
	PJ34 (60)	0.6 ± 0.08	1.0 ± 0.09	0.6
	DPQ (61)	4.5 ± 0.6	5.3 ± 0.5	0.8
	3	13 ± 0.15	0.8 ± 0.03	16.3
	19	8.0 ± 0.7	0.6 ± 0.2	13.3
	23	9.0 ± 0.7	0.9 ± 0.2	10.0

Table 3. (Continued)

Compound	IC ₅₀ [μM]		Selectivity PARP-1/PARP-2	
	PARP-1	PARP-2		
	44	10 ± 0.9	0.8 ± 0.06	12.5
	47	18 ± 1.9	9.0 ± 0.8	2.0
	51	3.0 ± 0.6	0.6 ± 0.2	5.0
	54	9.0 ± 0.7	0.15 ± 0.04	60.0
	55	8.0 ± 0.9	0.3 ± 0.08	26.7

[a] Data represent the mean ± SEM of at least three separate experiments conducted in duplicate.

scaffold **3** did not significantly alter the potency and selectivity profile of the parent compound, as all the derivatives studied are more potent at PARP-2, with selectivity indexes between 2 and 16.3. Interestingly, unsaturation of **3** to give the corresponding isoquinolinone derivative **54** enhanced PARP-2 inhibition, resulting in a selectivity index of 60. The same trend was confirmed for the acetophenone derivatives **44** and **55**, for which unsaturation of the dihydroisoquinolinone ring increased the selectivity index from 12.5 to 26.7.

To obtain data in whole cells we used fibroblasts from *PARP-1*^{-/-} and corresponding control *PARP-1*^{+/+} animals. The results show that whereas PJ34, a reference compound that inhibits both PARP-1 and PARP-2, decreases the enzymatic activity in both cell types, compound **55** at 10 μM decreases only PARP-2 (fibroblasts from *PARP-1*^{-/-}), leaving PARP-1 activity unchanged (Table 4).

Compd ^[b]	PARP-1 ^{+/+} [%] ^[c]	PARP-1 ^{-/-} [%] ^[c]
control	97 ± 3	102 ± 2
PJ34 (60)	21 ± 3	26 ± 2
55	88 ± 2.2	12 ± 3

[a] Data represent the mean ± SEM of at least three separate experiments conducted in duplicate. [b] Concentration: 10 μM. [c] Percentage of basal PARP activity in fibroblasts.

Discussion

The quest for selective PARP-1/PARP-2 inhibitors is motivated by the need for clarifying the different roles and the possible drugability of the two PARP isoforms under mild to severe genotoxic stimuli, along the road toward clinically useful agents. The high degree of similarity between the PARP-1 and PARP-2 catalytic domains (>90% identity in proximity of the NAD⁺ binding site) explains the difficulties so far encountered in developing isoform-selective inhibitors. Iwashita et al.^[14,15] reported a series of quinazolinone derivatives, exemplified by compound **1**, that have significant selectivity for PARP-1 over PARP-2 (IC₅₀^{PARP-2} = 500 nM; IC₅₀^{PARP-1} = 13 nM) and a series of quinoxaline derivatives, exemplified by compound **2**, with appreciable selectivity for PARP-2 over PARP-1 (IC₅₀^{PARP-1} = 100 nM; IC₅₀^{PARP-2} = 8 nM). The same authors provided a structural explanation for the observed selectivity profiles. Thus, the PARP-1-preferring quinazolinone inhibitor was co-crystallized with the human PARP-1 (hPARP-1) catalytic domain and docked in the homology model of the hPARP-2 catalytic domain. Despite a similar binding mode in the nicotinamide binding site, the preferential activity at PARP-1 was ascribed to a Leu/Gly substitution (Leu769_{PARP-1}/Gly314_{PARP-2}), resulting in a loss of hydrophobicity that prevents the side chain of the quinazolinone to bind PARP-2. Analogously, the PARP-2-preferential quinoxaline inhibitor was co-crystallized with the catalytic domain of hPARP-1 and docked in the homology model of hPARP-2. Again, the reason for the preferential activity toward PARP-2 was ascribed to the single Glu763/Gln308 mutation, resulting in an increased side chain mobility in PARP-2 that leads to optimal interaction with the distal *para*-chlorophenyl moiety of the quinoxaline derivative.

Herein we report the identification of compound **54** as a very selective PARP-2 inhibitor. With a selectivity index of 60, and an IC₅₀ value of 0.15 μM toward PARP-2, **54** is a very promising tool for studying the differential effect of transiently inhibiting PARP-2 versus PARP-1. With the aim of gaining insight into the structural basis for the preferential PARP-2 activity of the newly reported compounds, we carried out docking studies of compound **54** on a model of the catalytic domain of bovine PARP-1 built up by point mutations on the corresponding catalytic domain of human PARP-1 (PDB code: 1EFY), and on the catalytic domain of mouse PARP-2 (PDB code: 1GS0). Superimposition of the two catalytic domains reveals some differences in the proximity of the nicotinamide binding site (Figure 1).

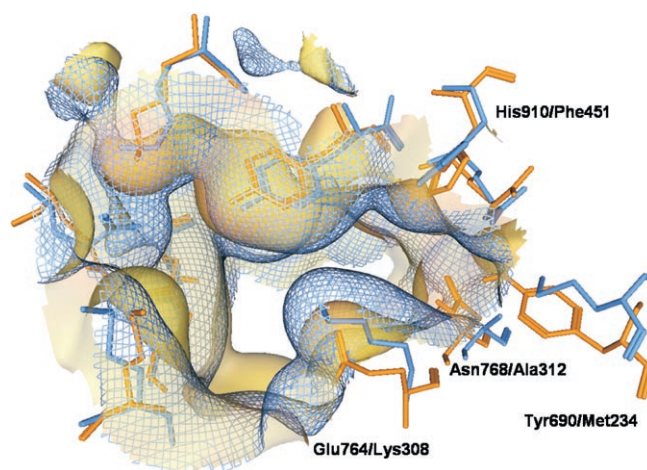


Figure 1. Superimposition of the catalytic sites of PARP-1 (orange) and PARP-2 (blue); non-conserved residues are labeled.

Most notably are the Glu764/Lys308, Asn768/Ala312, Tyr690/Met234, and His910/Phe451 substitutions (PARP-1/PARP-2 numbering). Interestingly, in mouse PARP-2, Lys308 substitutes the corresponding Gln308 in human PARP2, the residue used by Iwashita et al.^[14,15] to justify the PARP-2/PARP-1 selectivity observed in their quinoxaline series. While compound **54** adopted a similar conformation in both PARP-1 and PARP-2 catalytic sites, its benzoyl ester moiety is neatly projected into the PARP-2 cavity walled by Asp305, Lys306, Val307, and Lys308 (Figure 2). Notably, this conformation is potentially stabilized by the presence of a water molecule, which helps define the correct orientation of the inhibitor, thus forcing the benzoyl moiety into the PARP-2 cavity (Figure 2). Compound **3** showed an analogous pattern of interaction (Figure 2S, Supporting Information).

Conclusions

We report the preparation and preliminary evaluation of a library of isoquinolinone derivatives as potential PARP-2-selective inhibitors, and the identification of compound **54** as a potent PARP-2 inhibitor with 60-fold selectivity for PARP-2 over PARP-1. We thus demonstrated that selective inhibition of individual PARP isoforms can in fact be achieved through chemical manipulation of simple isoquinolinone derivatives bearing the 'canonical' PARP pharmacophore. Particularly intriguing is the notion that very subtle chemical modifications seem to govern PARP-1/PARP-2 selectivity. Compound **54** can therefore be considered a prototype tool for further *in vitro* and *in vivo* pharmacological characterizations of the involvement of PARP-2 in pathophysiological conditions.

Experimental Section

Chemistry: All general parallel syntheses as shown in Scheme 1 were carried out with a Carousel® apparatus (StepBio, Bologna, Italy) under controlled temperature and under argon atmosphere. Melting points were determined with a Büchi 535 electrothermal

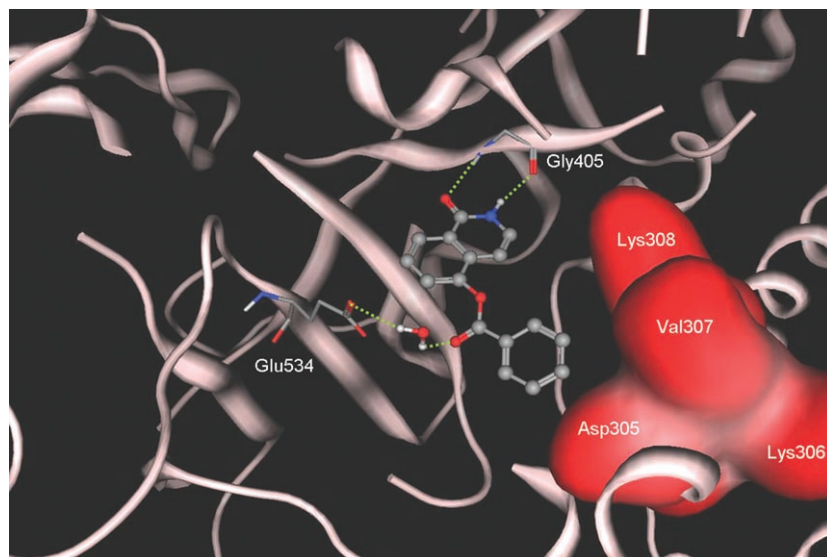


Figure 2. Docking pose of derivative **54** on mouse PARP2: residues defining the PARP-2 selectivity region are highlighted in red.

apparatus and are uncorrected. NMR spectra were obtained with a Bruker AC 200 or 400 MHz spectrometer, and the chemical shifts (δ) are reported in parts per million (ppm). The abbreviations used are as follows: s, singlet; d, doublet; dd, double doublet; dt, double triplet; m, multiplet; b, broad; p, pseudo. Flash column chromatography was performed using Merck silica gel 60 (0.040–0.063 mm). TLC was carried out on precoated TLC plates with silica gel 60 F_{254} (Merck). Spots were visualized by UV or by staining and warming with a phosphomolybdate reagent (5% in EtOH). Elemental analyses were carried out on a Carlo Erba 1106 analyzer. The analytical HPLC measurements were made on a Shimadzu LC workstation (Kyoto, Japan), class LC-8 A, equipped with an SPD-10Avp variable-wavelength UV/Vis detector and a Rheodyne 7725i injector with a stainless steel loop ($v=20\ \mu\text{L}$). The chromatographic traces were obtained with CLASS VP software (Shimadzu, v.4.3). The UV detection wavelength was set at 254 nm (first detection channel) and at 260 nm (second detection channel). All tested derivatives **3** and **19–59** showed high purity (see Supporting Information) in two different HPLC systems as well: a) column: Ultra Aqueous C_{18} (Restek, Bellefonte, PA, USA), $250\times 4.6\ \text{mm i.d.}$, $5\ \mu\text{m}$, $100\ \text{\AA}$; flow rate: $1.0\ \text{mL min}^{-1}$; eluent: NaH_2PO_4 buffer (10 mM, pH 7.4)/MeOH=3:7. b) column: LiChrospher 100 RP-18 (Merck, Darmstadt, Germany), $250\times 4.0\ \text{mm i.d.}$, $5\ \mu\text{m}$, $100\ \text{\AA}$; flow rate: $0.8\ \text{mL min}^{-1}$; eluent, $\text{H}_2\text{O}/\text{CH}_3\text{CN}=1:1$. Analytes were dissolved in DMSO and diluted with the eluent before HPLC injections; the analyses were performed at room temperature. Yields of final derivatives **3** and **19–59** refer to crystallized compounds and are not optimized.

General procedure A: NaOH (0.04 g, 1 mmol) was added to a solution of hydroxy derivative (1 mmol) in MeOH (5 mL), and held at reflux for 30 min. The reaction mixture was then evaporated under reduced pressure, and the residue was taken up with H_2O (12 mL). The residue was then opportunely divided in the Carousel tubes and treated with the suitable aryl chloride or bromide reagent (5 mmol) and $n\text{Bu}_4\text{NHSO}_4$ (0.02 mmol); the obtained suspension was heated overnight at 95°C . The reaction mixture was then acidified by $3\ \text{N HCl}$ and extracted with EtOAc. The organic layers were collected, washed with brine, dried over Na_2SO_4 , and evaporated under reduced pressure. The mixture was submitted to flash chromatography to obtain the desired derivatives. These com-

pounds were obtained as pure solids after crystallization in a mixture of EtOAc/*n*-hexane (~9:1).

General procedure B: K_2CO_3 (5 mmol) and the suitable halide reagent (1.2 mmol) were added to a solution of hydroxy derivative (1 mmol) in dry *N,N*-dimethylformamide (DMF, 5 mL), and the mixture was stirred in the Carousel tubes at room temperature for 16 h. H_2O (20 mL) was then added to the reaction mixture and extracted with EtOAc. The organic layers were collected, dried over Na_2SO_4 , and evaporated under reduced pressure. The mixture was submitted to flash chromatography to obtain the desired derivatives. These compounds were obtained as pure solids after crystallization in a mixture of EtOAc/*n*-hexane (~9:1).

Experimental data for compounds **4–9**, **11**, **14–17**, **20–22**, **24–43**, **45**, **46**, **48–50**, **52**, **53**, and **56–59** are reported in the Supporting Information.

5-Benzoyloxy-3,4-dihydroisoquinolin-1(2H)-one (3): Following general procedure A starting from 5-hydroxy-3,4-dihydroisoquinolin-1(2H)-one (**4**)^[18] (0.2 g, 1.22 mmol) and benzoyl chloride (0.86 g, 6.10 mmol), the title compound **3** was obtained as a pure solid (0.14 g, 44%); mp: $178\text{--}180^\circ\text{C}$; $^1\text{H NMR}$ (CDCl_3 , 400 MHz): $\delta=2.93$ (t, $J=6.6\ \text{Hz}$, 2H), 3.56 (dt, $J=1.9$ and $6.3\ \text{Hz}$, 2H), 6.45 (bs, 1H), 7.35–7.37 (m, 1H), 7.44 (t, $J=8.1\ \text{Hz}$, 1H), 7.53–7.57 (m, 2H), 7.66–7.70 (m, 1H), 8.05 (d, $J=7.7\ \text{Hz}$, 1H), 8.21–8.24 ppm (m, 2H); $^{13}\text{C NMR}$ (CDCl_3 , 100.6 MHz): $\delta=24.53$, 41.61, 127.93, 129.58, 130.74, 130.84, 132.23, 132.54, 133.42, 135.96, 149.48, 166.62, 167.52 ppm; anal. calcd for $\text{C}_{16}\text{H}_{13}\text{NO}_3$: C 71.90%, H 4.90%, N 5.24%, found: C 71.50%, H 4.63%, N 4.93%.

5-(2-Chlorobenzoyloxy)-3,4-dihydroisoquinolin-1(2H)-one (19): Following general procedure A starting from 5-hydroxy-3,4-dihydroisoquinolin-1(2H)-one (**4**)^[18] (0.2 g, 1.22 mmol) and 2-chlorobenzoylchloride (1.06 g, 6.1 mmol), the title compound **19** was obtained as a pure solid (0.161 g, 44%); mp: $174\text{--}175^\circ\text{C}$; $^1\text{H NMR}$ (CDCl_3 , 400 MHz): $\delta=2.97$ (t, $J=6.3\ \text{Hz}$, 2H), 3.59 (t, $J=6.2\ \text{Hz}$, 2H), 6.58 (bs, 1H), 7.38–7.46 (m, 3H), 7.51–7.57 (m, 2H), 8.06 ppm (t, $J=8.5$, 2H); $^{13}\text{C NMR}$ (CDCl_3 , 100.6 MHz): $\delta=22.56$, 39.53, 125.79, 126.08, 126.79, 127.58, 128.57, 130.43, 131.28, 131.46, 131.92, 133.48, 134.43, 147.19, 163.46, 165.54 ppm; anal. calcd for $\text{C}_{16}\text{H}_{12}\text{ClNO}_3$: C 63.69%, H 4.01%, N 4.64%, found: C 63.41%, H 3.98%, N 4.24%.

5-(3-Fluorobenzoyloxy)-3,4-dihydroisoquinolin-1(2H)-one (23): Following general procedure A starting from 5-hydroxy-3,4-dihydroisoquinolin-1(2H)-one (**4**)^[18] (0.2 g, 1.22 mmol) and 3-fluorobenzoylchloride (1.097 g, 6.1 mmol), the title compound **23** was obtained as a pure solid (0.065 g, 18%); mp: $148\text{--}149^\circ\text{C}$; $^1\text{H NMR}$ (CDCl_3 , 400 MHz): $\delta=2.92$ (t, $J=6.5\ \text{Hz}$, 2H), 3.57 (t, $J=6.3\ \text{Hz}$, 2H), 6.47 (bs, 1H), 7.35–7.46 (m, 3H), 7.53 (dt, $J=8.0$ and $5.4\ \text{Hz}$, 1H), 7.89 (dt, $J=2.3$ and $9.1\ \text{Hz}$, 1H), 8.01–8.07 ppm (m, 2H); $^{13}\text{C NMR}$ (CDCl_3 , 100.6 MHz): $\delta=22.44$, 39.54, 116.90 ($^2J_{\text{C-F}}=23.2\ \text{Hz}$), 121.02 ($^2J_{\text{C-F}}=21.3\ \text{Hz}$), 125.90, 127.59, 130.37 ($^3J_{\text{C-F}}=8.1\ \text{Hz}$), 130.84, 131.19, 147.18, 162.41 ($^1J_{\text{C-F}}=207.6\ \text{Hz}$), 163.81, 165.32 ppm; anal.

calcd for $C_{16}H_{12}FNO_3$: C 67.36%, H 4.24%, N 4.91%, found: C 67.12%, H 4.66%, N 4.65%.

5-(2-Oxo-2-phenylethoxy)-3,4-dihydroisoquinolin-1(2H)-one (44): Following general procedure B starting from 5-hydroxy-3,4-dihydroisoquinolin-1(2H)-one (**4**)^[18] (0.15 g, 0.92 mmol) and α -bromoacetophenone (0.27 g, 1.38 mmol), the title compound **44** was obtained as a pure solid (0.04 g, 16%); mp: 169–170 °C; ¹H NMR (CDCl₃, 400 MHz): δ = 3.09 (t, J = 6.7 Hz, 2H), 3.58 (dt, J = 2.5 and 6.7 Hz, 2H), 5.35 (s, 2H), 6.25 (bs, 1H), 6.93 (d, J = 8.2 Hz, 1H), 7.26 (t, J = 8.1 Hz, 1H), 7.5 (t, J = 7.9 Hz, 2H), 7.64 (t, J = 7.0 Hz, 1H), 7.74 (d, J = 7.8 Hz, 1H), 7.97–8.00 ppm (m, 2H); ¹³C NMR (CDCl₃, 100.6 MHz): δ = 23.06, 41.29, 72.53, 116.52, 122.47, 128.07, 129.42, 129.77, 130.32, 131.63, 135.44, 135.85, 155.64, 167.46, 195.41 ppm; anal. calcd for $C_{17}H_{15}NO_3$: C 72.58%, H 5.37%, N 4.98%, found: C 72.37%, H 5.10%, N 5.01%.

5-[2-(4-Cyanophenyl)-2-oxo-etoxy]-3,4-dihydroisoquinolin-1(2H)-one (47): Following general procedure B starting from 5-hydroxy-3,4-dihydroisoquinolin-1(2H)-one (**4**)^[18] (0.15 g, 0.92 mmol) and 4-cyano- α -bromoacetophenone (0.30 g, 1.38 mmol), the title compound **47** was obtained as a pure solid (0.09 g, 0.29 mmol, 32%); mp: 247–249 °C; ¹H NMR ([D₆]DMSO, 400 MHz): δ = 2.89 (t, J = 6.6 Hz, 2H), 3.35 (m, under H₂O 2H), 5.68 (s, 2H), 7.15 (d, J = 8.1 Hz, 1H), 7.24 (t, J = 8.0 Hz, 1H), 7.47 (d, J = 7.5 Hz, 1H), 7.92 (bs, 1H), 8.05 (d, J = 8.4 Hz, 2H), 8.15 ppm (d, J = 8.4 Hz, 2H); ¹³C NMR ([D₆]DMSO, 100.6 MHz): δ = 23.23, under [D₆]DMSO, 72.89, 117.09, 117.49, 119.97, 121.49, 128.76, 129.62, 130.43, 132.39, 134.70, 139.44, 155.87, 166.20, 195.96 ppm; anal. calcd for $C_{18}H_{14}N_2O_3$: C 70.58%, H 4.61%, N 9.15%, found: C 70.45%, H 4.78%, N 8.96%.

5-(Benzoisothiazol-3-yloxy)-3,4-dihydroisoquinolin-1(2H)-one (51): Following general procedure B starting from 5-hydroxy-3,4-dihydroisoquinolin-1(2H)-one (**4**)^[18] (0.1 g, 0.61 mmol) and 2-chlorobenzoisothiazole (0.12 g, 0.73 mmol), the title compound **51** was obtained as a pure solid (0.05 g, 28%); mp: 225–227 °C; ¹H NMR ([D₆]DMSO, 400 MHz): δ = 3.05 (t, J = 6.3 Hz, 2H), 4.02 (t, J = 6.3 Hz, 2H), 7.05 (d, J = 8.0 Hz, 1H), 7.20 (t, J = 8.0 Hz, 1H), 7.33–7.42 (m, 3H), 7.66 (t, J = 7.7 Hz, 1H), 7.87 (d, J = 7.5 Hz, 1H), 9.92 ppm (bs, 1H); ¹³C NMR ([D₆]DMSO, 100.6 MHz): δ = 24.42, 55.29, 107.78, 117.79, 120.92, 121.03, 126.14, 128.36, 128.49, 129.20, 131.01, 135.85, 135.98, 144.46, 155.63, 167.53 ppm; anal. calcd for $C_{16}H_{16}N_2O_2S$: C 64.85%, H 4.08%, N 9.45%, found: C 65.02%, H 4.29%, N 9.08%.

5-Benzoyloxyisoquinolin-1(2H)-one (54): Following general procedure B starting from 5-hydroxyisoquinolin-1(2H)-one (**5**)^[20] (0.1 g, 0.62 mmol) and benzoyl chloride (0.11 g, 0.09 mL, 0.74 mmol), the title compound **54** was obtained as a pure solid (0.04 g, 24.3%); mp: 233–235 °C; ¹H NMR ([D₆]DMSO, 400 MHz): δ = 6.39 (d, J = 7.2 Hz, 1H), 7.19 (t, J = 6 Hz, 1H), 7.55 (t, J = 7.9 Hz, 1H), 7.63–7.69 (m, 3H), 7.79 (t, J = 7.4 Hz, 1H), 8.14 (d, J = 8 Hz, 1H), 8.21 (dd, J = 1.4 and 7.1 Hz, 2H), 11.43 ppm (bs, 1H); ¹³C NMR ([D₆]DMSO, 100.6 MHz): δ = 99.69, 126.63, 127.53, 128.29, 129.32, 130.20, 131.04, 131.82, 132.10, 133.10, 136.27, 147.28, 163.04, 166.39 ppm; anal. calcd for $C_{16}H_{11}NO_3$: C 72.45%, H 4.18%, N 5.28%, found: C 72.31%, H 3.98%, N 5.02%.

5-[2-Oxo-etoxy-2-phenyl]-isoquinolin-1(2H)-one (55): Following general procedure B starting from 5-hydroxyisoquinolin-1(2H)-one (**5**)^[20] (0.075 g, 0.46 mmol) and 2-bromoacetophenone (0.111 g, 0.56 mmol), the title compound **55** was obtained as a pure solid (0.03 g, 23.3%); mp: 166–168 °C; ¹H NMR ([D₆]DMSO, 400 MHz): δ = 5.73 (s, 2H), 6.79 (d, J = 7.1 Hz, 1H), 7.17–7.21 (m, 2H), 7.35 (t, J = 8.0 Hz, 1H), 7.57 (t, J = 7.6 Hz, 2H), 7.69–7.75 (m, 2H), 8.04 (d, J = 7.5 Hz, 2H), 11.29 ppm (bs, 1H); ¹³C NMR ([D₆]DMSO, 100.6 MHz):

δ = 72.60, 100.61, 115.24, 120.57, 128.34, 129.06, 129.77, 130.27, 130.51, 130.72, 135.73, 136.24, 154.54, 163.33, 196.07 ppm; anal. calcd for $C_{17}H_{13}NO_3$: C 73.11%, H 4.69%, N 5.02%, found: C 72.81%, H 4.78%, N 5.07%.

Molecular modeling: All studies were carried out as fully reported elsewhere.^[24,25]

Biology: measurement of PARP activity in vitro: Given that pure human PARP-1/PARP-2 enzymes are not commercially available, bovine recombinant PARP-1 and mouse recombinant PARP-2 activity was assayed according to Banasik et al.^[22] Briefly, the enzymatic reaction was carried out in a final volume of 100 μ L. The reaction mixture, containing bovine serum albumin (0.5 μ g μ L⁻¹), Tris-HCl (100 mM, at pH 7.4 for PARP-1 and at pH 8.0 for PARP-2), MgCl₂ (20 mM), dithiothreitol (5 mM), calf thymus DNA (20 μ g, sonicated 45 s), NAD⁺ (10 μ M), [2,8-³H-adenine]NAD⁺ (35.5 nM, 0.2 μ Ci), recombinant enzyme (0.05 U), and various concentrations of the compounds dissolved in DMF, was incubated at 37 °C for 60 min. The reaction was stopped by adding trichloroacetic acid (10%, 1 mL), and the radioactivity incorporated from [2,8-³H-adenine]-NAD⁺ into proteins was evaluated by liquid scintillation counting. Measurement of PARP activity on *PARP-1*^{-/-} and *PARP-1*^{+/+} fibroblasts were performed as reported elsewhere.^[26]

Statistical analysis: Dose–response curves of PARP inhibitors were analyzed, and IC₅₀ values were calculated with the Prism software package (GraphPad Software Inc., San Diego, CA, USA). Statistical significance of differences between results was evaluated by ANOVA plus Turkey's post hoc test.

Supporting Information available: Experimental chemical data for compounds **4–9**, **11**, **14–17**, **20–22**, **24–43**, **45**, **46**, **48–50**, **52**, **53**, and **56–59**; experimental HPLC data for compounds **3** and **19–59**; curves of compounds **3** and **54** used to generate their IC₅₀ values; figure of compound **3** in the docking experiment.

Acknowledgements

This work was co-financed by grants from the Italian Ministry of Research (MIUR) PRIN 2004 and PRIN 2006. We are also grateful to Wyeth (Princeton, USA) for financial support.

Keywords: isoquinolinones · medicinal chemistry · molecular docking · PARP-2 inhibitors · poly(ADP-ribosylation)

- [1] V. Schreiber, F. Dantzer, J. C. Ame, G. de Murcia, *Nat. Rev. Mol. Cell Biol.* **2006**, *7*, 517–528.
- [2] A. Chiarugi, *Trends Pharmacol. Sci.* **2002**, *23*, 122–129.
- [3] R. Pellicciari, E. Camaioni, G. Costantino, *Prog. Med. Chem.* **2004**, *42*, 125–169.
- [4] G. Graziani, C. Szabo, *Pharmacol. Res.* **2005**, *52*, 109–118.
- [5] M. J. Eliasson, K. Sampei, A. S. Mandir, P. D. Hurn, R. J. Traystman, J. Bao, A. Pieper, Z. Q. Wang, T. M. Dawson, S. H. Snyder, V. L. Dawson, *Nat. Med.* **1997**, *3*, 1089–1095.
- [6] W. M. Shieh, J. C. Ame, M. V. Wilson, Z. Q. Wang, D. W. Koh, M. K. Jacobson, E. L. Jacobson, *J. Biol. Chem.* **1998**, *273*, 30069–30072.
- [7] J. C. Ame, V. Rolli, V. Schreiber, C. Niedergang, F. Apiou, P. Decker, S. Muller, T. Hoger, J. M. de Murcia, G. de Murcia, *J. Biol. Chem.* **1999**, *274*, 17860–17868.
- [8] S. Shall, G. de Murcia, *Mutat. Res.* **2000**, *460*, 1–15.
- [9] M. Endres, Z. Q. Wang, S. Namura, C. Waeber, M. A. Moskowitz, *J. Cereb. Blood Flow Metab.* **1997**, *17*, 1143–1151.

- [10] J. Kofler, T. Otsuka, Z. Zhang, R. Noppens, M. R. Grafe, D. W. Koh, V. L. Dawson, J. M. de Murcia, P. D. Hurn, R. J. Traystman, *J. Cereb. Blood Flow Metab.* **2006**, *26*, 135–141.
- [11] A. Huber, P. Bai, J. M. de Murcia, G. de Murcia, *DNA Repair* **2004**, *3*, 1103–1110.
- [12] J. Yélamos, Y. Monreal, L. Saenz, E. Aguado, V. Schreiber, R. Mota, T. Fuente, A. Minguela, P. Parrilla, G. de Murcia, E. Almarza, P. Aparicio, M. J. de Murcia, *EMBO J.* **2006**, *25*, 4350–4360.
- [13] F. Dantzer, M. Mark, D. Quenet, H. Scherthan, A. Huber, B. Liebe, L. Monaco, A. Chicheportiche, P. Sassone-Corsi, G. de Murcia, M. J. de Murcia, *Proc. Natl. Acad. Sci. USA* **2006**, *103*, 14854–14859.
- [14] A. Iwashita, K. Hattori, H. Yamamoto, J. Ishida, Y. Kido, K. Kamijo, K. Murano, H. Miyake, T. Kinoshita, M. Warizaya, M. Ohkubo, N. Matsuoka, S. Mutoh, *FEBS Lett.* **2005**, *579*, 1389–1393.
- [15] J. Ishida, H. Yamamoto, Y. Kido, K. Kamijo, K. Murano, H. Miyake, M. Ohkubo, T. Kinoshita, M. Warizaya, A. Iwashita, K. Mihara, N. Matsuoka, K. Hattori, *Bioorg. Med. Chem.* **2006**, *14*, 1378–1390.
- [16] A. Chiarugi, E. Meli, M. Calvani, R. Picca, R. Baronti, E. Camaioni, G. Costantino, M. Marinozzi, D. E. Pellegrini-Giampietro, R. Pellicciari, F. Moroni, *J. Pharmacol. Exp. Ther.* **2003**, *305*, 943–949.
- [17] R. Pellicciari, E. Camaioni, G. Costantino, M. Marinozzi, A. Macchiarulo, F. Moroni, B. Natalini, *Farmaco* **2003**, *58*, 851–858.
- [18] M. J. Suto, W. R. Turner, C. M. Arundel-Suto, L. M. Werbel, J. S. Sebolt-Leopold, *Anticancer Drug Des.* **1991**, *6*, 107–117.
- [19] Y. Miyake, H. Shimadzu, N. Hashimoto, Y. Ishida, M. Shibakawa, T. Nishimura, *J. Labelled Compd. Radiopharm.* **2000**, *43*, 983–988.
- [20] V. Georgian, R. J. Harrison, L. L. Skaletzky, *J. Org. Chem.* **1962**, *27*, 4571–4579.
- [21] T. Nakatani, E. Nishimura, N. Noda, *J. Nat. Med.* **2006**, *60*, 261–263.
- [22] M. Banasik, H. Komura, M. Shimoyama, K. Ueda, *J. Biol. Chem.* **1992**, *267*, 1569–1575.
- [23] G. E. Albdelkarim, K. Gertz, C. Harms, J. Katchanov, U. Dirnagl, C. Szabó, M. Endres, *Int. J. Mol. Med.* **2001**, *7*, 255–260.
- [24] G. Costantino, A. Macchiarulo, E. Camaioni, R. Pellicciari, *J. Med. Chem.* **2001**, *44*, 3786–3794.
- [25] D. Bellocchi, A. Macchiarulo, G. Costantino, R. Pellicciari, *Bioorg. Med. Chem.* **2005**, *13*, 1151–1157.
- [26] S. Fossati, L. Formentini, Z. Q. Wang, F. Moroni, A. Chiarugi, *Biochem. Cell Biol.* **2006**, *84*, 703–712.

Received: January 16, 2008

Revised: March 13, 2008

Published online on April 11, 2008